Order, disorder and dynamics in brownmillerite $Sr_2Fe_2O_5$

Josie E. Auckett, Wai Tung Lee, Kirrily C. Rule, Alexey Bosak and Chris D. Ling

SUPPORTING INFORMATION

Theory of polarised neutron scattering

The possible choices of oppositely polarised states for the incident and analysed neutron beams give rise to two oppositely polarised non-spin-flip (NSF) configurations, "plus-plus" (++) and "minus-minus" (– –), and two spin-flip (SF) configurations, "plus-minus" (+–) and "minus-plus" (–+). When the guide magnetic field is aligned perpendicular to the scattering vector, the scattered intensity measured in the NSF modes is defined by the following equations:

$$I_{(++)} \propto N^2 + M_L{}^2 + 2NM_L \qquad (1)$$
$$I_{(--)} \propto N^2 + M_L{}^2 - 2NM_L \qquad (2)$$

where I is the total scattering intensity, N is the nuclear scattering contribution and M_L is the longitudinal magnetic scattering contribution (parallel to the guide field but perpendicular to the scattering vector q). The opposite SF scattering intensities are always equal except in chiral magnetic structures, and obey the relation

$$I_{SF} \propto M_T{}^2 \qquad (3)$$

where M_T is the transverse magnetic scattering contribution (perpendicular to the guide field and to q).

When the guide magnetic field is parallel to the scattering vector, the NSF scans contain only nuclear scattering intensity ($M_L = 0$), and the SF signal includes all magnetic scattering contributions in the plane perpendicular to H and q.

Polarised neutron scattering experiment on the $Sr_2Fe_2O_5$ crystal: Additional notes

Figure S1 demonstrates the effect of the polarisation intensity correction[1] applied to the raw diffraction intensities measured for the purely nuclear (080) reflection. After the correction, the (++) and (– –) curves are almost indistinguishable and spurious intensity of the (+ –) peak intensity is eliminated.

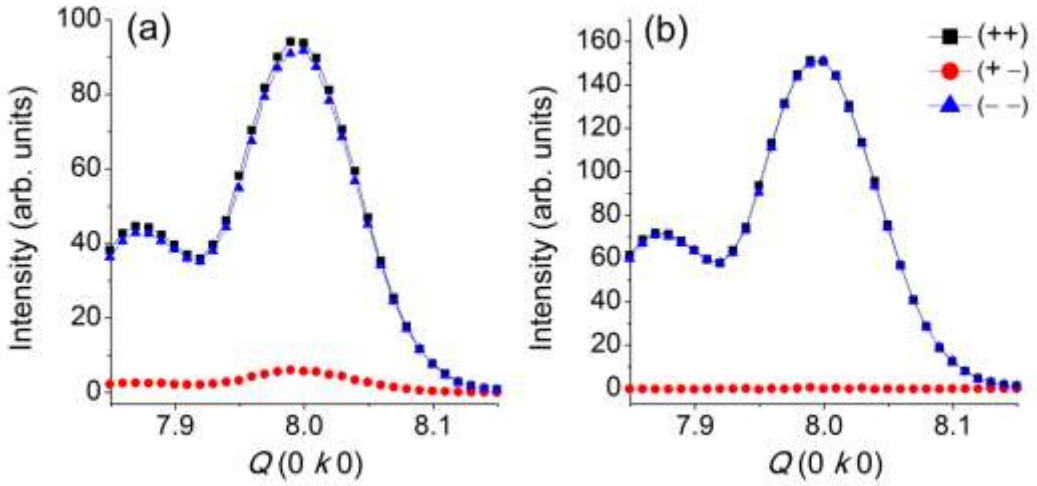

Figure S1. Polarised neutron diffraction data near the (080) reflection, (a) before and (b) after applying a correction for polarisation decay. Image (b) corresponds to Figure 4(a) in the manuscript. Error bars are smaller than symbols.

Following from equations (1)–(3) given in the previous section, equality of $I_{(++)}$ and $I_{(--)}$ combined with significant I_{SF} intensity in the (H ⊥ q) condition is indicative of purely magnetic scattering (N = 0). This was found to be the case for the reflections (231), (251) and (271). For these magnetic peaks, the relations given in equations (1) and (3) allow the relative contributions of M_L and M_T to be determined from the ratio of (++) and (+–) intensities measured with H ⊥ q, so that the angle of the magnetic moment projected on the plane perpendicular to q can be pinpointed by considering these intensities at multiple reflections. The measured reflections (231), (251) and (271) were therefore used to determine the angles ϕ_0 (between [201] and the projection of the magnetic moment m on the scattering plane) and α (between m and H), using the equation

$$\tan\theta(k) = \frac{\boldsymbol{m}\cdot\boldsymbol{p}}{\boldsymbol{m}\cdot\boldsymbol{H}} = \frac{\sin(\phi_0+\phi(k))\sin\alpha}{\cos\alpha} = \sin(\phi_0+\phi(k))\tan\alpha \qquad (4)$$

where p is the direction perpendicular to H and q, and θ is the measured angle between H and the projection of the magnetic moment m on the scattering plane (see Figure S2). The resulting values of α = 44.8° and ϕ_0 = 1.8° yield two possible solutions for the spin direction, corresponding within the level of experimental accuracy to the [100] and [001] directions. This finding is consistent with the known antiferromagnetic structure of $Sr_2Fe_2O_5$ where the spins aligned parallel and anti-parallel to [001], although unambiguous confirmation of this model by polarised neutron scattering would require the consideration of additional reflection intensities measured in a different scattering plane.

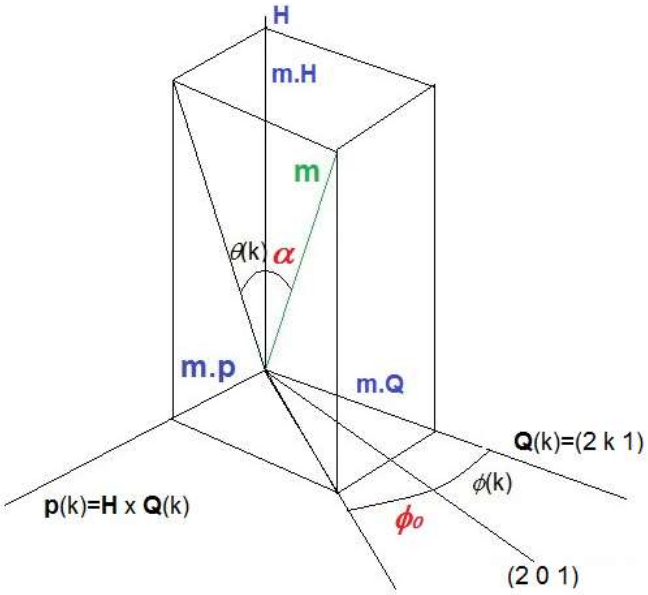

Figure S2. Scattering geometry used to pinpoint *m* by calculating its angles of deviation from H and [201].

Additional synchrotron diffraction data

Figure S3 presents selected precession images reconstructed from the MX1 data set collected for a $Sr_2Fe_2O_5$ at 100 K. In contrast to the planes shown in the manuscript Figure 5, the twinned diffraction patterns recorded in these planes can be reproduced adequately using a non-modulated brownmillerite unit cell with *Icmm* symmetry, as they do not contain any of the additional reflections caused by doubling of the *a* axis in the chain-ordered *Pbma* supercell.

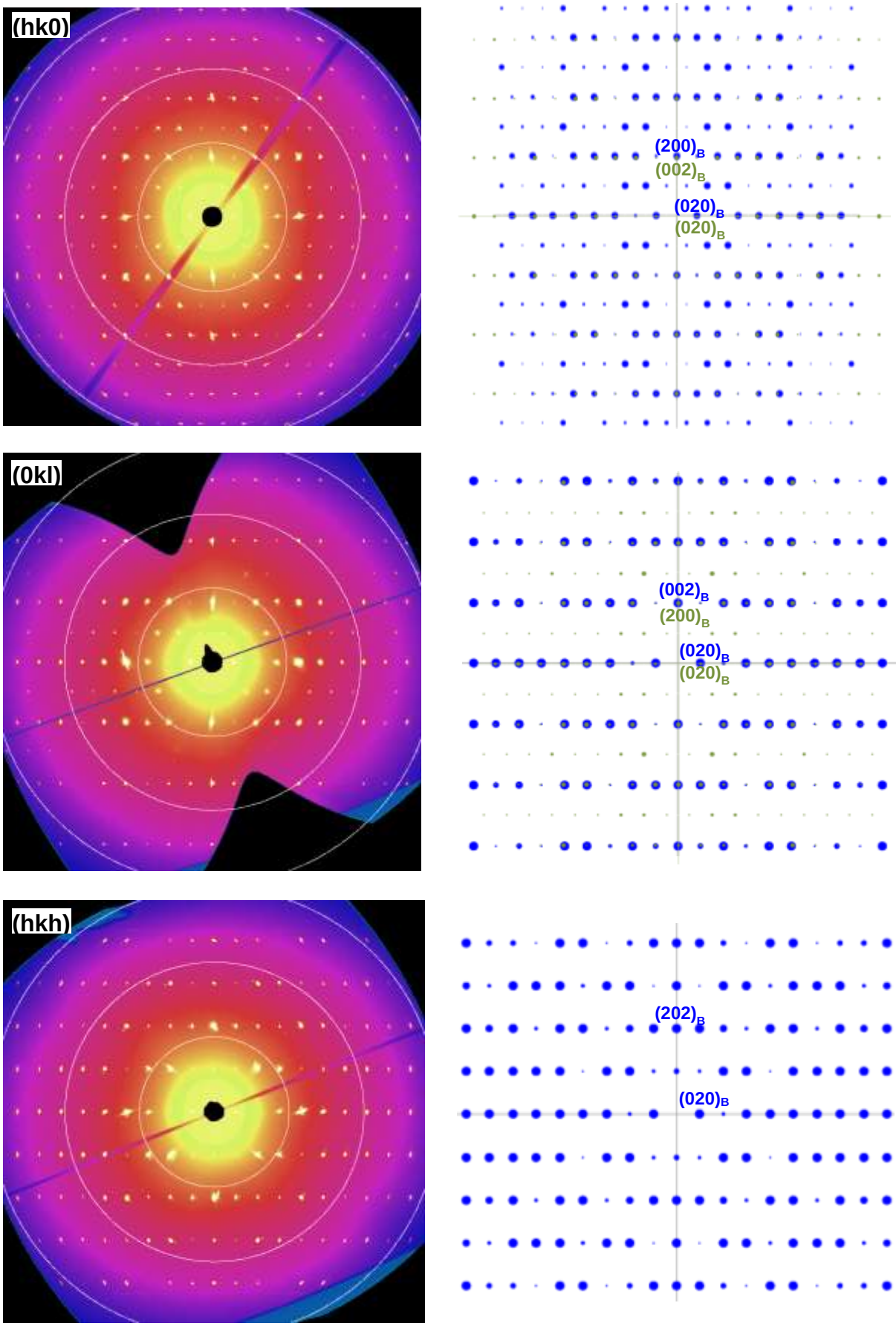

Figure S3. (Left) Synchrotron x-ray (MX1) precession images of $Sr_2Fe_2O_5$. (Right) Diffraction maps calculated for the *Icmm* subcell model. Blue and green maps represent two different twin contributions, for which index labels are positioned above and below the corresponding reflections, respectively. Plane labels on the left-hand images refer to the blue component.

Precession images were also generated from the deliberately over-saturated ID23 data set in the (*hk*0), (*h*0*l*) and (2*h k h*) planes. The visual patterns of Bragg reflections corresponded closely to those of the MX1 precession images in every plane, confirming the same basic structure model and twinning behaviour in both crystals. Strong streaks of diffuse scattering were clearly evident in the [010]* directions of (*hk*0) and (2*h k h*), and in the ⟨201⟩* directions of (*h*0*l*) and (2*h k h*) (Figure S4). These directions correspond to ⟨100⟩$_P$-type directions in the simple cubic perovskite unit cell from which brownmillerite is derived, and are also the directions along which the micro-crystals in the FZ-grown boule are twinned. Local disorder at the boundaries between microtwin domains therefore offers a plausible explanation for the observed diffuse features.

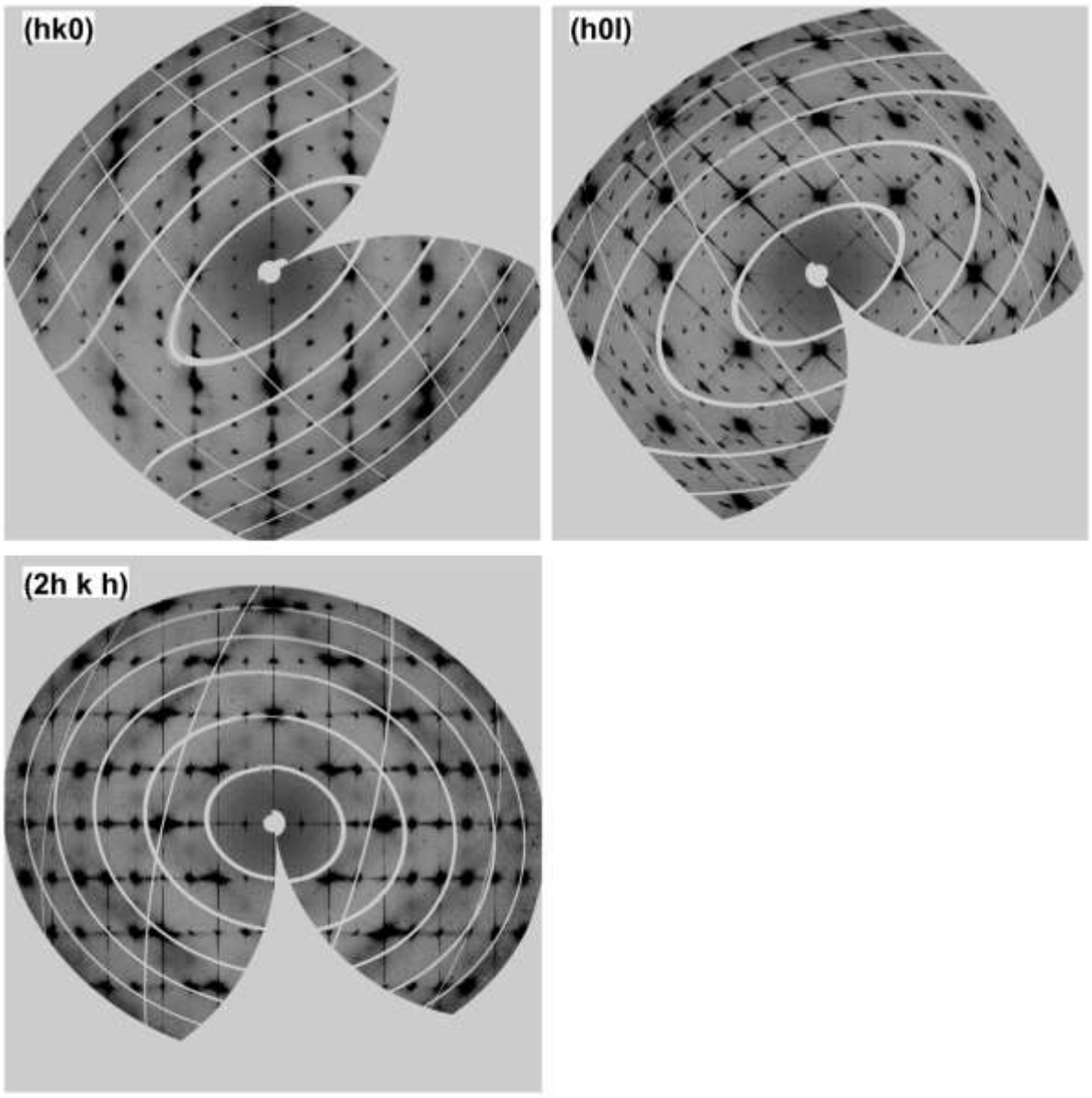

Figure S4. Precession images generated for $Sr_2Fe_2O_5$ from the high-intensity ID23 synchrotron x-ray diffraction data.

(1) Wildes, A. R. The polarizer-analyzer correction problem in neutron polarization analysis experiments. *Rev. Sci. Instrum.* **1999,** *70* (11), 4241-4245.